

**Effect of atomic-hydrogen irradiation on reduction of residual carrier  
concentration in  $\beta$ -FeSi<sub>2</sub> films grown on Si substrates by  
atomic-hydrogen-assisted molecular beam epitaxy**

Y. Funase, M. Suzuno, K. Toko, and T. Suemasu

Institute of Applied Physics, University of Tsukuba, Tsukuba, Ibaraki 305-8573, Japan

**Corresponding author:** T. Suemasu

Institute of Applied Physics, University of Tsukuba, Tsukuba, Ibaraki 305-8573, Japan

TEL/FAX: +81-29-853-5311, Email: [suemasu@bk.tsukuba.ac.jp](mailto:suemasu@bk.tsukuba.ac.jp)

$\beta$ -FeSi<sub>2</sub> films were epitaxially grown by atomic-hydrogen-assisted molecular beam epitaxy (MBE) on high-resistive *n*-type floating-zone (FZ) Si(111) ( $\rho > 1000 \Omega\cdot\text{cm}$ ). They showed *n*-type conduction with a reduced electron concentration of an order of  $10^{16} \text{ cm}^{-3}$  at room temperature (RT). In contrast,  $\beta$ -FeSi<sub>2</sub> films prepared without atomic hydrogen or prepared with molecular hydrogen showed *p*-type conduction with a large hole density of over  $10^{18} \text{ cm}^{-3}$ . These results show that the atomic-hydrogen irradiation is an effective means to reduce the residual carrier concentration in undoped  $\beta$ -FeSi<sub>2</sub> films.

Keywords: A3. Molecular beam epitaxy; A3. Atomic hydrogen; B2. Semiconducting silicide; B1.  $\beta$ -FeSi<sub>2</sub>; A1. Residual carrier concentration

## 1. Introduction

Semiconducting  $\beta$ -FeSi<sub>2</sub> has a bandgap of approximately 0.78 eV [1,2], corresponding to optical fiber communication wavelengths. In addition, it has a very larger optical absorption coefficient of over  $10^5$  cm<sup>-1</sup> at 1 eV [3]. For the past 20 years, there have been numerous reports on the development of infrared light-emitting diodes and detectors using  $\beta$ -FeSi<sub>2</sub> [4-9]. In particular, a photoresponsivity of over 100 mA/W for 1.31  $\mu$ m light for *n*-type  $\beta$ -FeSi<sub>2</sub> single crystals has spurred interest in this material [10,11]. However, the highest photoresponsivity obtained so far for  $\beta$ -FeSi<sub>2</sub> thin films (6 mA/W at 1.31  $\mu$ m) is still more than one order of magnitude smaller than that for *n*-type  $\beta$ -FeSi<sub>2</sub> single crystals [12]. One of the reasons for small photoresponsivity in  $\beta$ -FeSi<sub>2</sub> films is a large residual carrier concentration, and thereby a small minority-carrier lifetime. Regarding the residual carrier concentration, it is well known that the conduction type of  $\beta$ -FeSi<sub>2</sub> depends on the atomic ratio of Si to Fe [13-16]. Tani and Kido performed first-principles calculations of defects in  $\beta$ -FeSi<sub>2</sub> using density functional theory. They showed that Si vacancies have lower formation energies than Fe vacancies in  $\beta$ -FeSi<sub>2</sub> and that crystals containing Si vacancies exhibit *p*-type conduction [17]. Al doping has been reported to be an effective way to substitute for Si vacancies [18]. However, there have been only a few reports on methods to reduce the residual

carrier concentration in  $\beta$ -FeSi<sub>2</sub>. Terai *et al.* achieved carrier concentrations of the order of  $10^{16} \text{ cm}^{-3}$  by precisely controlling the growth conditions in molecular-beam epitaxy (MBE) [19]. Very recently, we successfully decreased the residual carrier concentrations by MBE using a cracking cell for generating atomic hydrogen [20]. The conduction type changed from *p*- to *n*-type and the carrier concentration was two orders of magnitude (of an order of  $n \approx 10^{16} \text{ cm}^{-3}$ ) lower than that for films grown in the absence of atomic hydrogen. However, the conduction type of the Si substrate used was *n*-type, the same as that of  $\beta$ -FeSi<sub>2</sub> films prepared with atomic hydrogen. Thus, we cannot exclude the influence of the Si substrate on the measured carrier concentrations. In addition, the effect of molecular hydrogen has not been made clear. In this article, we aimed to add the experimental results to our previous results [24], and to clarify the effect of atomic hydrogen on the  $\beta$ -FeSi<sub>2</sub> films.

## 2. Experimental

$\beta$ -FeSi<sub>2</sub> films were epitaxially grown by a two-step growth method including reactive deposition epitaxy (RDE; Fe deposition on hot Si) and MBE (codeposition of Fe and Si) on 500- $\mu\text{m}$ -thick *n*-type floating-zone (FZ) Si(111) substrates ( $\rho > 1000 \text{ }\Omega\text{-cm}$ ), and on silicon-on-insulator (SOI) substrates with approximately 0.7- $\mu\text{m}$ -thick

(111)-oriented FZ Si layers ( $\rho > 1000 \text{ } \Omega \cdot \text{cm}$ ). Here, the SOI substrate was fabricated by bonding together the FZ-Si(111) substrate and a quartz substrate. Following bonding, the Si substrate was thinned to approximately  $0.7 \text{ } \mu\text{m}$  by grinding mechanically and by chemical mechanical polishing processes. The growth procedure for  $\beta\text{-FeSi}_2$  films is the same as that used previously [21]. Briefly, 20-nm-thick  $\beta\text{-FeSi}_2$  template layers were formed at  $650 \text{ } ^\circ\text{C}$  by RDE, followed by MBE at  $750 \text{ } ^\circ\text{C}$ . Atomic hydrogen was generated by heating a tungsten filament at  $1800 \text{ } ^\circ\text{C}$ ; the substrate was continuously irradiated with atomic hydrogen during growth. The cracking efficiency of the atomic hydrogen source was approximately 3% at  $1800 \text{ } ^\circ\text{C}$  [22]. The beam equivalent pressure,  $P_{\text{H}_2}$ , of hydrogen was kept constant during growth, but it was varied from sample to sample as follows: 0 Pa (samples A and E),  $8 \times 10^{-6}$  Pa (sample B),  $8 \times 10^{-5}$  Pa (samples C and F), and  $8 \times 10^{-4}$  Pa (sample D). For sample, G hydrogen was supplied during the growth but the cracking was not carried out, meaning that molecular hydrogen was supplied. The samples were prepared as summarized in Table 1.

Reflection high-energy electron diffraction (RHEED), and X-ray diffraction (XRD) were used to characterize the crystalline quality of the grown films. The carrier concentration and mobility were measured at RT by the van der Pauw method. The applied magnetic field was 0.54 T normal to the sample surface. Ohmic contacts were

formed on the surfaces of  $\beta$ -FeSi<sub>2</sub> with Au/Cr.

### 3. Results and discussion

Figure 1 shows the photograph of the SOI substrate we fabricated. The Si layer thickness around the center region was less than 0.7  $\mu\text{m}$ . The sheet resistance of the Si increased up to more than 10 M $\Omega$ . Since this sheet resistance is approximately 700 times greater than that of the 500- $\mu\text{m}$ -thick *n*-FZ-Si, we would expect to see differences in carrier concentrations between samples AC and EF if the influence of current flow in the *n*-Si substrate is not negligibly small. Figures 2(a) and 2(b) present the  $\theta$ -2 $\theta$  XRD and RHEED patterns observed along the Si[1-10] azimuth for sample E grown without atomic hydrogen, and for sample F, grown with  $P_{\text{H}_2}=8\times 10^{-5}$  Pa on the SOI substrates. The diffraction peaks from (110) or (101)-oriented  $\beta$ -FeSi<sub>2</sub> are dominant. This orientation of  $\beta$ -FeSi<sub>2</sub> relative to the Si(111) surface is consistent with the epitaxial relationship between the two materials [23]. These figures exhibited that the  $\beta$ -FeSi<sub>2</sub> films were epitaxially grown on the SOI substrates. Similar results were obtained for the other samples.

Next, we discuss the results of Hall measurements. Figures 3(a) and 3(b) show the dependences of carrier concentration and carrier mobility in  $\beta$ -FeSi<sub>2</sub> films (samples

A–G), respectively, measured at RT on  $P_{\text{H}_2}$ . Sample A had a hole concentration  $p$  of  $3.0 \times 10^{19} \text{ cm}^{-3}$  and hole mobility  $\mu_{\text{h}}$  of  $3.0 \text{ cm}^2/\text{V}\cdot\text{s}$ . The  $\beta\text{-FeSi}_2$  film in sample B, prepared with  $P_{\text{H}_2}=8 \times 10^{-6} \text{ Pa}$ , still showed  $p$ -type conductivity, but the  $p$  value decreased a little down to  $1.9 \times 10^{18} \text{ cm}^{-3}$ , and the  $\mu_{\text{h}}$  value was increased to  $60 \text{ cm}^2/\text{V}\cdot\text{s}$ . When  $P_{\text{H}_2}$  was increased further to  $8 \times 10^{-5} \text{ Pa}$  in sample C, the conductivity changed from  $p$ - to  $n$ -type, and the electron concentration  $n$  decreased significantly to the range between  $7.8 \times 10^{16}$  and  $4.6 \times 10^{17} \text{ cm}^{-3}$ . Furthermore, the  $n$  value decreased to  $1.3 \times 10^{16}$ – $3.0 \times 10^{17} \text{ cm}^{-3}$  in sample D when  $P_{\text{H}_2}$  was increased further from  $8 \times 10^{-5} \text{ Pa}$  to  $8 \times 10^{-4} \text{ Pa}$ . Regarding the electron mobility  $\mu_{\text{e}}$  in samples C and D, they did not show a steady increase with decreasing  $n$ , but rather tended to scatter. The excess hydrogen supply degrades the crystalline quality of  $\beta\text{-FeSi}_2$  [20], and thereby carriers are supposed to be scattered due to various scattering mechanisms [24]. In samples C and D, we cannot eliminate the possibility that the  $500\text{-}\mu\text{m}$ -thick  $n$ -Si substrate influenced the measured  $n$  and  $\mu_{\text{e}}$  values, because the carrier type of  $\beta\text{-FeSi}_2$  in these samples is the same as in the Si substrate used.

Thus, we next carried out Hall measurements on samples E and F, grown on the SOI substrates. Sample E, grown without a hydrogen supply, shows  $p$ -type conductivity, the same as sample A. Sample F, grown with  $P_{\text{H}_2}=8 \times 10^{-5} \text{ Pa}$ , revealed  $n$ -type

conductivity, and the  $n$  and  $\mu_e$  values were  $8.9 \times 10^{16} \text{ cm}^{-3}$  and  $\mu_e = 85 \text{ cm}^2/\text{V}\cdot\text{s}$ , respectively. These values are close to those in sample C, meaning that the influence of the  $n$ -Si substrate was not so significant that the measured  $n$  and  $\mu_e$  values in samples C and D are valid. Finally we discussed the effect of molecular hydrogen on the reduction of carrier concentration. For sample G, the hydrogen was supplied, but the cracking was not performed. The  $\beta$ -FeSi<sub>2</sub> in this sample showed  $p$ -type conductivity with a large  $p$  value more than  $10^{18} \text{ cm}^{-3}$ . On the basis of these results, it can at least be stated that the carrier concentration decreased drastically for  $\beta$ -FeSi<sub>2</sub> grown by MBE not with molecular hydrogen but with atomic hydrogen.

#### 4. Summary

We have grown  $\beta$ -FeSi<sub>2</sub> films by atomic hydrogen-assisted MBE on Si(111) substrates, and on SOI substrates with 0.7- $\mu\text{m}$ -thick Si layers with a (111) orientation. It was found from Hall measurements that atomic hydrogen irradiation was a very effective means in reducing the carrier concentration of  $\beta$ -FeSi<sub>2</sub>. The films showed  $n$ -type conductivity with an electron concentration of the order of  $10^{16} \text{ cm}^{-3}$  when  $P_{\text{H}_2}$  was  $8 \times 10^{-4} \text{ Pa}$  during film growth. The reduction in carrier concentration was not observed in  $\beta$ -FeSi<sub>2</sub> films prepared with molecular hydrogen.

## References

- [1] K. Takakura, N. Hiroi, T. Suemasu, S. F. Chichibu, F. Hasegawa, *Appl. Phys. Lett.* 80 (2002) 556.
- [2] H. Udono, I. Kikuma, T. Okuno, Y. Masumoto, H. Tajima, *Appl. Phys. Lett.* 85 (2004) 1937.
- [3] M. C. Bost, J. E. Mahan, *J. Appl. Phys.* 58 (1985) 2696.
- [4] K. Lefki, P. Muret, *J. Appl. Phys.* 74 (1993) 1138.
- [5] D. Leong, M. Harry, K. J. Reeson, K. P. Homewood, *Nature* 387 (1997) 686.
- [6] Y. Maeda, T. Akita, K. Umezawa, K. Miyake, M. Sagawa, *Proc. SPIE* 3419 (1998) 354.
- [7] T. Suemasu, Y. Negishi, K. Takakura, F. Hasegawa, *Jpn. J. Appl. Phys.* 39 (2000) L1013.
- [8] M. Suzuno, T. Koizumi, T. Suemasu, *Appl. Phys. Lett.* 94 (2009) 213509.
- [9] M. Shaban, K. Nomoto, S. Izumi, T. Yoshitake, *Appl. Phys. Lett.* 94 (2009) 222113.
- [10] T. Ootsuka, T. Suemasu, J. Chen, T. Sekiguchi, *Appl. Phys. Lett.* 92 (2008) 042117.
- [11] T. Ootsuka, T. Suemasu, J. Chen, T. Sekiguchi, Y. Hara, *Appl. Phys. Lett.* 92 (2008) 192114.

- [12] M. Shaban, T. Yoshitake, *Advances in Photodiodes* (InTech Open Access Publisher, March 2011), Chap. 1, 315-330.
- [13] M. Komabayashi, K. Hijikata, S. Ido, *Jpn. J. Appl. Phys.* 29 (1990) 1118.
- [14] T. Miki, Y. Matsui, K. Matsubara, K. Kishimoto, *J. Appl. Phys.* 75 (1994) 1693.
- [15] T. Miki, Y. Matsui, Y. Teraoka, Y. Ebina, K. Matsubara, K. Kishimoto, *J. Appl. Phys.* 76 (1994) 2097.
- [16] K. Takakura, T. Suemasu, Y. Ikura, F. Hasegawa, *Jpn. J. Appl. Phys.* 39 (2000) L789.
- [17] J. Tani, H. Kido, *J. Alloys Compd.* 352 (2003) 153.
- [18] Y. Terai, Y. Maeda, *Appl. Phys. Lett.* 84 (2004) 903.
- [19] Y. Terai, K. Yoneda, K. Noda, N. Miura, Y. Fujiwara, *J. Appl. Phys.* 112 (2012) 013702.
- [20] K. Akutsu, H. Kawakami, M. Suzuno, T. Yaguchi, K. Jiptner, J. Chen, T. Sekiguchi, T. Ootsuka, T. Suemasu, *J. Appl. Phys.* 109 (2011) 123502.
- [21] M. Takauji, N. Seki, T. Suemasu, F. Hasegawa, M. Ichida, *J. Appl. Phys.* 96 (2004) 2561.
- [22] A. Sutoh, Y. Okada, S. Ohta, M. Kawabe, *Jpn. J. Appl. Phys.* 34 (1995) L1379.
- [23] K. M. Geib, J. E. Mahan, R. G. Long, M. Nathan, G. Bai, *J. Appl. Phys.* 70 (1991)

1730.

[24] M. Suzuno, Y. Ugajin, S. Murase, T. Suemasu, M. Uchikoshi, M. Isshiki, J. Appl.

Phys. 102 (2007) 103706.

Fig. 1 Photograph of the SOI substrate we formed. The Si layer thickness around the center is less than  $0.7 \mu\text{m}$ .

Fig. 2  $\theta$ - $2\theta$  XRD and RHEED patterns observed along the Si[1-10] azimuth for sample E, grown without atomic hydrogen, and for sample F, grown with  $P_{\text{H}_2}=8\times 10^{-5}$  Pa on the SOI substrates. The forbidden diffraction peak of Si(222) indicated by asterisk occurs by double diffraction

Fig. 3 Dependences of (a) carrier type and carrier concentration, and (b) carrier mobility in  $\beta$ -FeSi<sub>2</sub> films (samples A–G) measured at RT on  $P_{\text{H}_2}$ .

Table 1. Sample preparation: substrate,  $P_{\text{H}_2}$  during hydrogen irradiation, and growth thicknesses of RDE and MBE-grown  $\beta\text{-FeSi}_2$  layers. Carrier type, carrier density and mobility are also shown.

Sample	Substrate	$P_{\text{H}_2}$ (Pa)	RDE/MBE (nm)	Carrier density ( $\text{cm}^{-3}$ )	Mobility ( $\text{cm}^2/\text{V}\cdot\text{s}$ )
A	FZ- <i>n</i> -Si(111)	w/o	20/560	$p=3.0\times 10^{19}$	1.3
B	FZ- <i>n</i> -Si(111)	$8\times 10^{-6}$	20/480	$p=1.8\times 10^{18}$	60
C	FZ- <i>n</i> -Si(111)	$8\times 10^{-5}$	20/260	$n=7.8\times 10^{16}$	130
D	FZ- <i>n</i> -Si(111)	$8\times 10^{-4}$	20/560	$p=1.3\times 10^{16}$	330
E	SOI	w/o	20/590	$p=3.8\times 10^{18}$	2.3
F	SOI	$8\times 10^{-5}$	20/510	$n=8.9\times 10^{16}$	85
G	FZ- <i>n</i> -Si(111)	$8\times 10^{-5}$ ( $\text{H}_2$ )	20/360	$p=4.3\times 10^{18}$	8.8

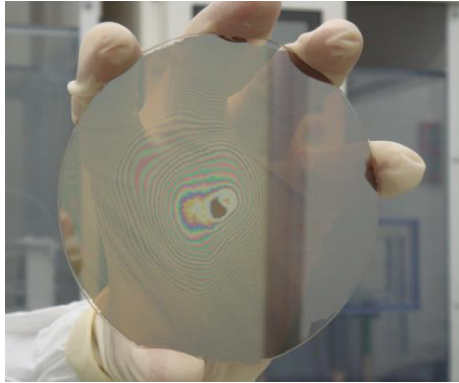


Fig. 1

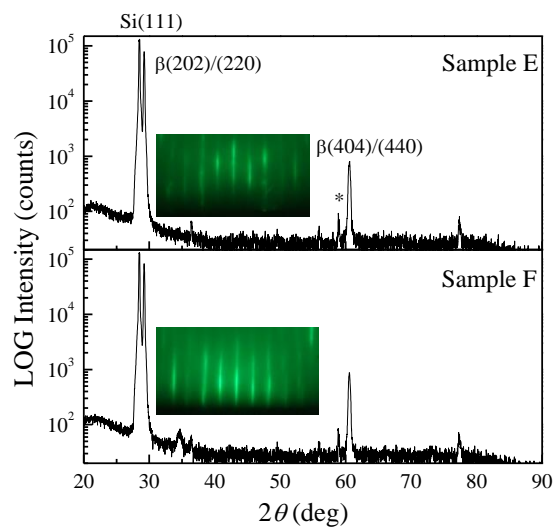


Fig. 2

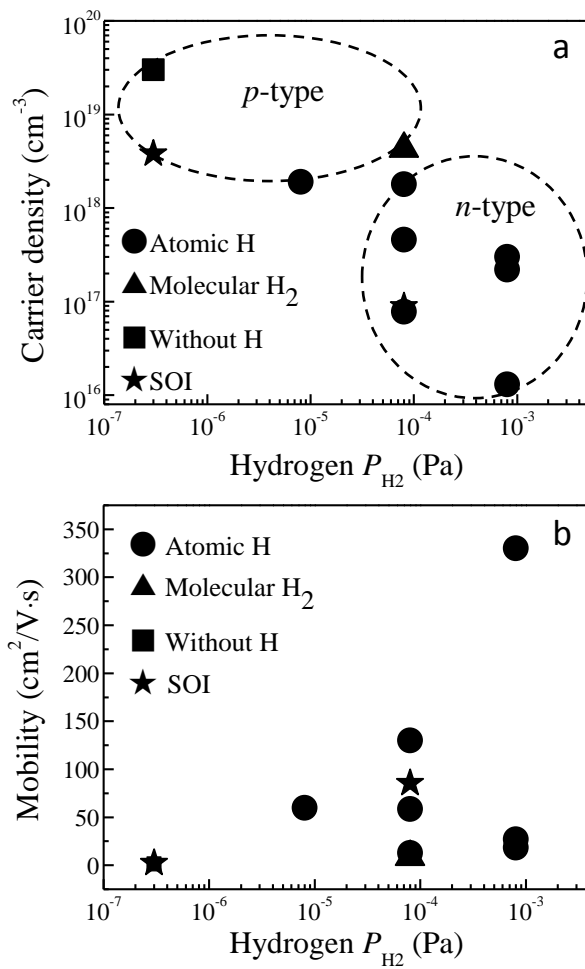


Fig. 3